

A higher order virtual element method for the Cahn-Hilliard equation

Alice Hodson, Andreas Dedner

Mathematics Institute, University of Warwick, Coventry, UK
alice-rachel.hodson@warwick.ac.uk

WARWICK
THE UNIVERSITY OF WARWICK

Cahn-Hilliard equation

Introduced by Cahn and Hilliard to model phase separation, the two dimensional Cahn-Hilliard equation is given as follows

$$\partial_t u - \Delta(\phi(u) - \varepsilon^2 \Delta u) = 0 \quad \text{in } \Omega \times (0, T], \quad (1a)$$

$$u(\cdot, 0) = u_0(\cdot) \quad \text{in } \Omega, \quad (1b)$$

$$\partial_n u = 0, \partial_n(\phi(u) - \varepsilon^2 \Delta u) = 0 \quad \text{on } \partial\Omega \times (0, T], \quad (1c)$$

for time $T > 0$. We define $\phi(x) = \psi'(x)$, where the free energy $\psi : \mathbb{R} \rightarrow \mathbb{R}$ is given by

$$\psi(x) := \frac{1}{4}(1 - x^2)^2$$

- ◊ We study a nonconforming VEM spatial discretisation cf. [1]
- ◊ We present the first higher order method without using a mixed formulation of equation (1)

Continuous and semi-discrete problems

Find $u(\cdot, t) \in V = H_0^2(\Omega)$ such that

$$(\partial_t u, v) + \varepsilon^2(D^2 u, D^2 v) + r(u; u, v) = 0 \quad \forall v \in V \quad (2)$$

$$u(\cdot, 0) = u_0(\cdot) \in V$$

where the semilinear form $r(\cdot; \cdot, \cdot)$ is defined as

$$r(z; v, w) = \int_{\Omega} \phi'(z) Dv \cdot Dw \, dx \quad \forall z, v, w \in V.$$

Find $u_h(\cdot, t) \in V_{h,\ell}$ such that

$$m_h(\partial_t u_h, v_h) + \varepsilon^2 a_h(u_h, v_h) + r_h(\Pi_0^K(u_h); u_h, v_h) = 0 \quad \forall v_h \in V_{h,\ell} \quad (3)$$

$$u_h(\cdot, 0) = u_{h,0}(\cdot) \in V_{h,\ell}$$

Virtual element discretisation

- Using the VEM construction in [2] our local nonconforming virtual element space is constructed so that $V_{h,\ell}^K \subset \tilde{V}_{h,\ell}^K$ for some enlarged space $\tilde{V}_{h,\ell}^K$
- The discrete forms m_h, a_h , and r_h are built using the following computable projection operators

$$\text{Value projection: } \Pi_0^K : \tilde{V}_{h,\ell}^K \rightarrow \mathbb{P}_\ell(K)$$

$$\text{Gradient projection: } \Pi_1^K : \tilde{V}_{h,\ell}^K \rightarrow [\mathbb{P}_{\ell-1}(K)]^2$$

$$\text{Hessian projection: } \Pi_2^K : \tilde{V}_{h,\ell}^K \rightarrow [\mathbb{P}_{\ell-2}(K)]^{2 \times 2}$$

- Denoting the orthogonal $L^2(K)$ -projection onto the polynomial space $\mathbb{P}_k(K)$ by \mathcal{P}_k^K , the projections satisfy the following crucial property

$$\Pi_s^K w_h = \mathcal{P}_{\ell-s}^K(D^s w_h) \quad \forall w_h \in V_{h,\ell}^K, \quad \text{for } s = 0, 1, 2$$

- The local virtual element space $V_{h,\ell}^K$ is then defined using the projections and is characterised by the following set of unisolvent degrees of freedom

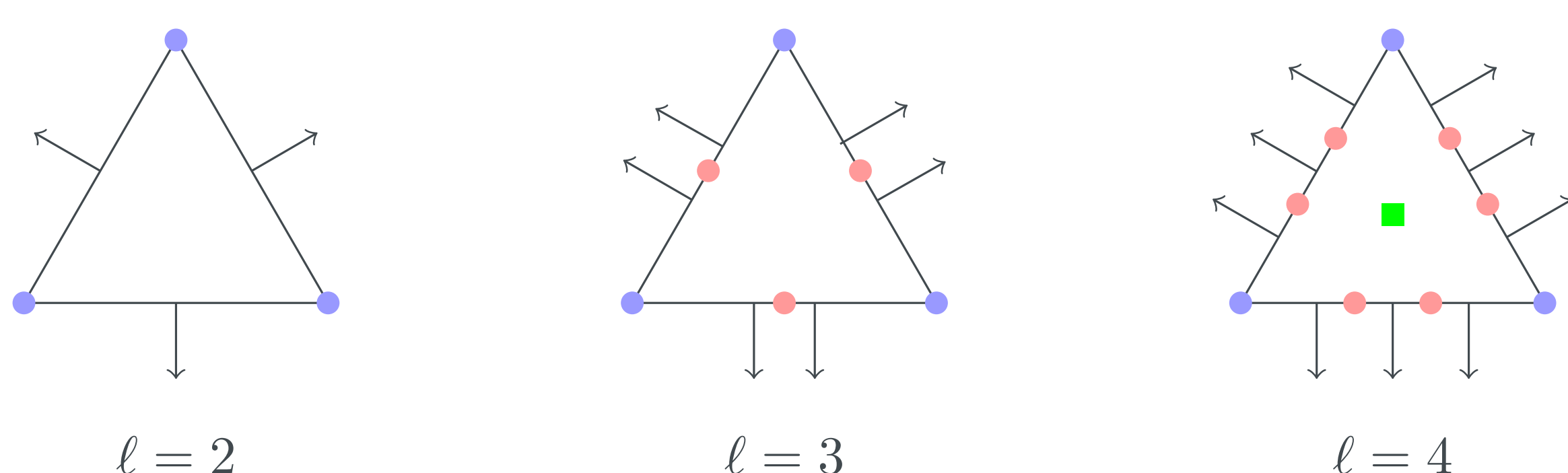


Figure 1: Degrees of freedom on triangles. Circles at vertices represent vertex evaluation, arrows represent edge normal moments, circles on edges represent edge value moments and squares represent inner moments

Main result: L^2 convergence theorem

Assume that u is the solution to the continuous problem (2) and u_h is the solution to (3). Then, for all $t \in [0, T]$,

$$\|u - u_h\|_{0,h} \lesssim h^\ell \quad (4)$$

Test 1: Convergence to an exact solution

Table 1: We verify the convergence result (4) by setting the forcing so that the exact solution is given by $u(x, y, t) = \sin(2\pi t) \cos(2\pi x) \cos(2\pi y)$. We present the L^2 errors and eocs for the lowest order ($\ell = 2$) VEM discretisation coupled with a second order Runge-Kutta time stepping method

size	dofs	h	L^2 error	L^2 eoc
25	128	0.3288	1.9833e-01	—
100	503	0.1535	4.6127e-02	1.92
400	2003	0.0751	1.0867e-02	2.02
1600	8003	0.0402	2.5869e-03	2.29

Test 2: Evolution of a cross

- We monitor the evolution of initial data relating to a cross-shaped interface between phases

$$u_0(x, y) = \begin{cases} 0.95 & \text{if } |(y - \frac{1}{2}) - \frac{2}{5}(x - \frac{1}{2})| + |\frac{2}{5}(x - \frac{1}{2}) + (y - \frac{1}{2})| < \frac{1}{5}, \\ 0.95 & \text{if } |(x - \frac{1}{2}) - \frac{2}{5}(y - \frac{1}{2})| + |\frac{2}{5}(y - \frac{1}{2}) + (x - \frac{1}{2})| < \frac{1}{5}, \\ -0.95 & \text{otherwise.} \end{cases}$$

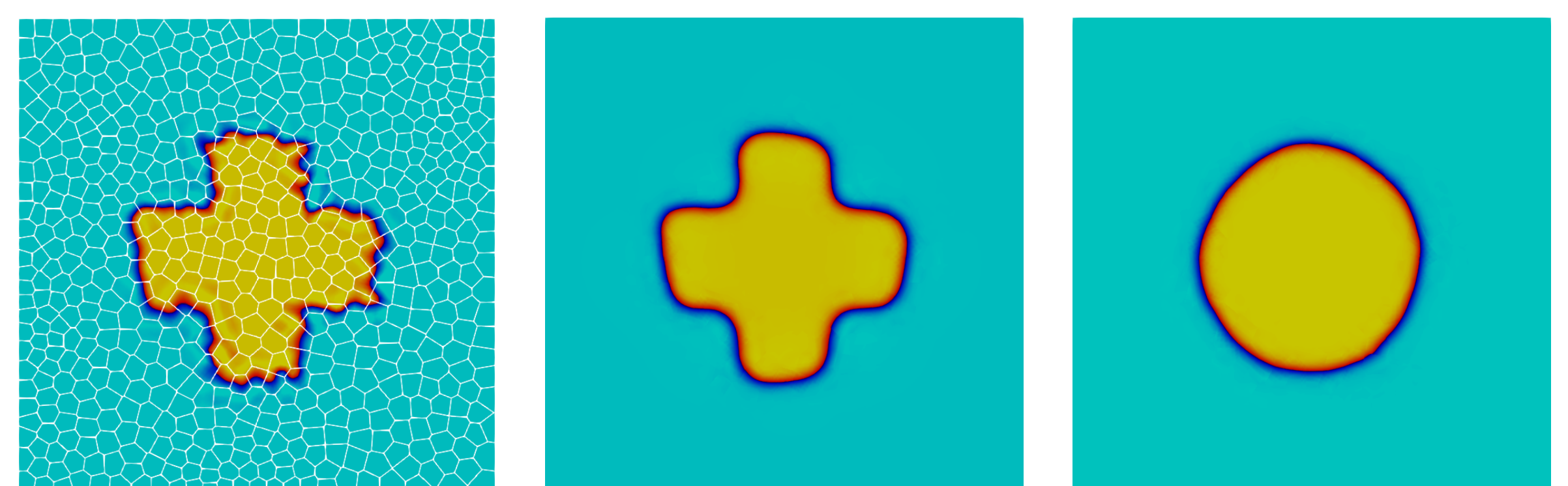


Figure 2: Snapshots of test 2 on a polygonal Voronoi grid at the time frames from left to right ($t = 0, 0.004, 0.8$)

Test 3: Spinodal decomposition

- We monitor the evolution of initial data taken to be a random perturbation between -1 and 1 located in the centre of the domain

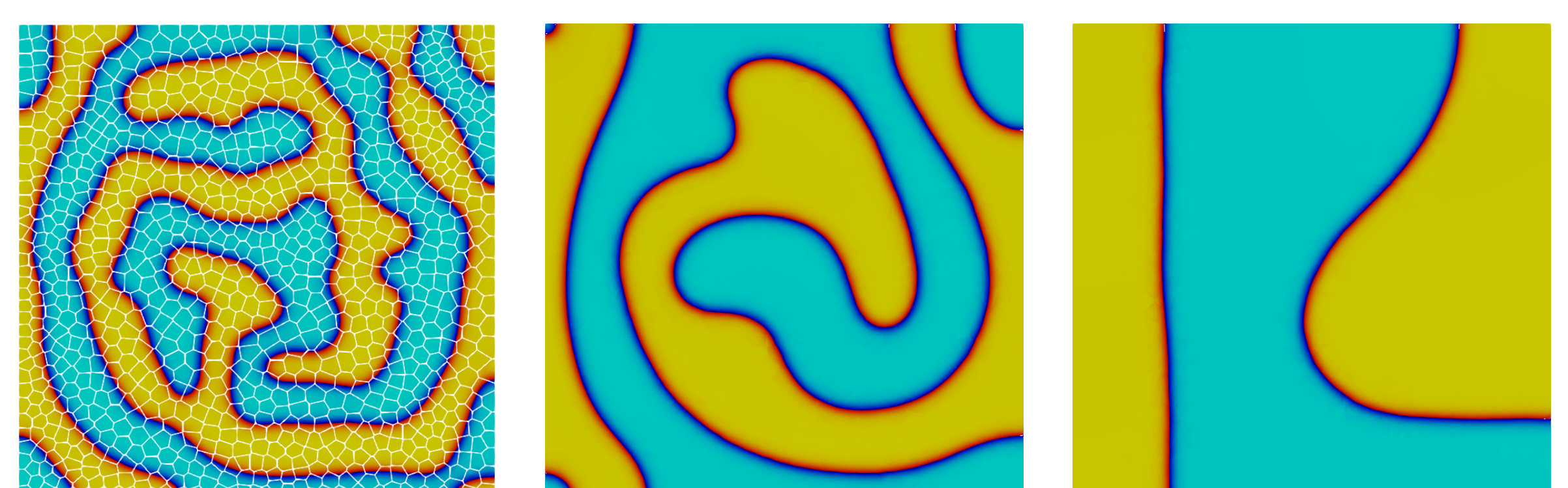


Figure 3: Snapshots of test 3 on a polygonal Voronoi grid at the time frames from left to right ($t = 0.04, 0.4, 5$)

References

- (1) A. Dedner and A. Hodson, *arXiv preprint arXiv:2111.11408*, 2021.
- (2) A. Dedner and A. Hodson, *IMA J. Numer. Anal.*, 2021, drab003, DOI: 10.1093/imanum/drab003.